

RESEARCH ARTICLE

Generation and phenotypic characterization of *Pde1a* mutant mice

Xiaofang Wang¹, Satsuki Yamada², Wells B. LaRiviere¹, Hong Ye¹, Jason L. Bakeberg³, María V. Irazabal¹, Fouad T. Chebib¹, Jan van Deursen⁴, Peter C. Harris^{1,4}, Caroline R. Sussman¹, Atta Behfar², Christopher J. Ward^{3*}, Vicente E. Torres^{1*}

1 Division of Nephrology and Hypertension, Mayo Clinic, Rochester, Minnesota, United States of America, **2** Department of Cardiovascular Diseases, Mayo Clinic, Rochester, Minnesota, United States of America, **3** Division of Nephrology and Hypertension, University of Kansas Medical Center, Kansas City, Kansas, United States of America, **4** Department of Biochemistry and Molecular Biology, Mayo Clinic, Rochester, Minnesota, United States of America

* Torres.vicente@mayo.edu (VET); cward6@kumc.edu (CJW)



OPEN ACCESS

Citation: Wang X, Yamada S, LaRiviere WB, Ye H, Bakeberg JL, Irazabal MV, et al. (2017) Generation and phenotypic characterization of *Pde1a* mutant mice. PLoS ONE 12(7): e0181087. <https://doi.org/10.1371/journal.pone.0181087>

Editor: Giovanna Valenti, Università degli Studi di Bari Aldo Moro, ITALY

Received: March 31, 2017

Accepted: June 26, 2017

Published: July 27, 2017

Copyright: © 2017 Wang et al. This is an open access article distributed under the terms of the [Creative Commons Attribution License](https://creativecommons.org/licenses/by/4.0/), which permits unrestricted use, distribution, and reproduction in any medium, provided the original author and source are credited.

Data Availability Statement: All relevant data are within the paper and its Supporting Information files.

Funding: This study was funded by the National Institutes of Health (DK44863 and DK90728) and by the Mayo Clinic Robert M. and Billie Kelley Pirnie Translational PKD Research Center. VET is PI for DK44863 and DK90728 and Director of the Mayo Clinic Robert M. and Billie Kelley Pirnie Translational PKD Research Center. CJW was Co-Investigator in the same grants. PCH is Co-Investigator in the same grants and Co-Director of

Abstract

It has been proposed that a reduction in intracellular calcium causes an increase in intracellular cAMP and PKA activity through stimulation of calcium inhibitable adenylyl cyclase 6 and inhibition of phosphodiesterase 1 (PDE1), the main enzymes generating and degrading cAMP in the distal nephron and collecting duct, thus contributing to the development and progression of autosomal dominant polycystic kidney disease (ADPKD). In zebrafish *pde1a* depletion aggravates and overexpression ameliorates the cystic phenotype. To study the role of PDE1A in a mammalian system, we used a TALEN pair to *Pde1a* exon 7, targeting the histidine-aspartic acid dipeptide involved in ligating the active site Zn⁺⁺ ion to generate two *Pde1a* null mouse lines. *Pde1a* mutants had a mild renal cystic disease and a urine concentrating defect (associated with upregulation of PDE4 activity and decreased protein kinase A dependent phosphorylation of aquaporin-2) on a wild-type genetic background and aggravated renal cystic disease on a *Pkd2*^{WS25/-} background. *Pde1a* mutants additionally had lower aortic blood pressure and increased left ventricular (LV) ejection fraction, without a change in LV mass index, consistent with the high aortic and low cardiac expression of *Pde1a* in wild-type mice. These results support an important role of PDE1A in the renal pathogenesis of ADPKD and in the regulation of blood pressure.

Introduction

Autosomal dominant polycystic kidney disease (ADPKD) is the fourth leading cause of end-stage kidney disease. It is caused by mutations in *PKD1* or *PKD2* encoding polycystin 1 and polycystin 2 [1, 2]. Substantial evidence supports the hypothesis that disruption of polycystin function results in dysregulation of intracellular calcium dynamics and upregulation of 3',5'-cyclic adenosine monophosphate (cAMP) and protein kinase A (PKA) signaling [3–5]. The identification of cAMP and PKA signaling as a therapeutic target [6–9] has led to clinical trials of vasopressin V2 receptor (V2R) antagonists and somatostatin analogs [10, 11] and to the

the Mayo Clinic Robert M. and Billie Kelley Pirnie Translational PKD Research Center. The funders had no role in study design, data collection and analysis, decision to publish, or preparation of the manuscript.

Competing interests: The authors have declared that no competing interests exist.

recent approval of the V2R antagonist, tolvaptan, for the treatment of ADPKD with rapidly progressive renal disease in Japan, Canada, the European Union, Switzerland and South Korea.

Further understanding of the mechanisms responsible for the increased cAMP signaling in PKD may provide additional therapeutic opportunities. It has been proposed that the increase in cAMP signaling is, in part, a direct consequence of a reduction in intracellular calcium homeostasis through the inhibition of phosphodiesterase (PDE)-1, the only PDE activated by calcium [6]. The PDE1 family consists of three isoforms encoded by three distinct genes, *PDE1A*, *PDE1B* and *PDE1C*. We have shown that *pde1a* interference using splice- and translation-blocking morpholinos causes pronephric cysts, hydrocephalus, and body curvature in wild-type zebrafish embryos and aggravates the cystic phenotype in *pkd2* morphants, while human *PDE1A* RNA partially rescues the *pde1a* and *pkd2* morphant phenotypes [12]. To study the role of PDE1A in a mammalian system we created Pde1a null mouse lines using TALENs.

Methods

The Mayo Clinic Institutional Animal Care and Utilization Committee approved all experimental protocols for the work described within this report.

Targeted disruption of *Pde1a*

We used a TALEN pair to *Pde1a* exon 7 (NM_001159582.1 mouse chromosome 2). This exon was selected because it is the second exon in the catalytic domain and contains a histidine-aspartic acid dipeptide involved in the coordination of a Zn⁺⁺ ion required for catalytic activity [13] (Fig 1A). We injected a total of 100 C57BL6/J oocytes, recovered 40 pups of which at least 5 males and 3 females harbored a mutation.

Genotyping and breeding of *Pde1a* and *Pkd2* mutant mice

Pde1a (Fig A in S1 File) and *Pkd2* genotyping by PCR and Southern blot are described in the Supplemental material. *Pde1a*^{Del15/Del15}, *Pkd2*^{+/-} and *Pkd2*^{WS25/WS25} mice were crossed to generate *Pde1a*^{Del15/Del15};*Pkd2*^{-/WS25} and *Pde1a*^{+/+};*Pkd2*^{-/WS25} mice.

Phenotypic characterization of *Pde1a* mutant mice

Litter sizes, blood and urine biochemistries and magnetic resonance imaging (MRI) of the abdomen and/or heart were obtained at 6 and 12 months in *Pde1a* mutant and wild-type mice. Urinary concentrating ability and the capacity to excrete a water load were tested at 12 months of age. Echocardiogram, aortic blood pressure and histology of *Pde1a*^{Del15/Del15} and *Pde1a*^{InsA/InsA} were compared to those of sex and age matched wild-type controls.

Treatment with desmopressin

Desmopressin (30 ng/100 g/hour) or saline vehicle was administered subcutaneously via osmotic minipumps (Alzet 1004 replaced every 3 wk) to wild-type and *Pde1a*^{InsA/InsA} mice, or to wild-type;*Pkd2*^{-/WS25} and *Pde1a*^{Del15/Del15};*Pkd2*^{-/WS25} mice between 4 and 16 weeks of age.

Abdominal and cardiac MRI

Ultra high field (UHF) abdominal and cardiac MRI images were acquired as described in the supplemental material (<https://www.jove.com/video/52757/use-ultra-high-field-mri-small-rodent-models-polycystic-kidney>).

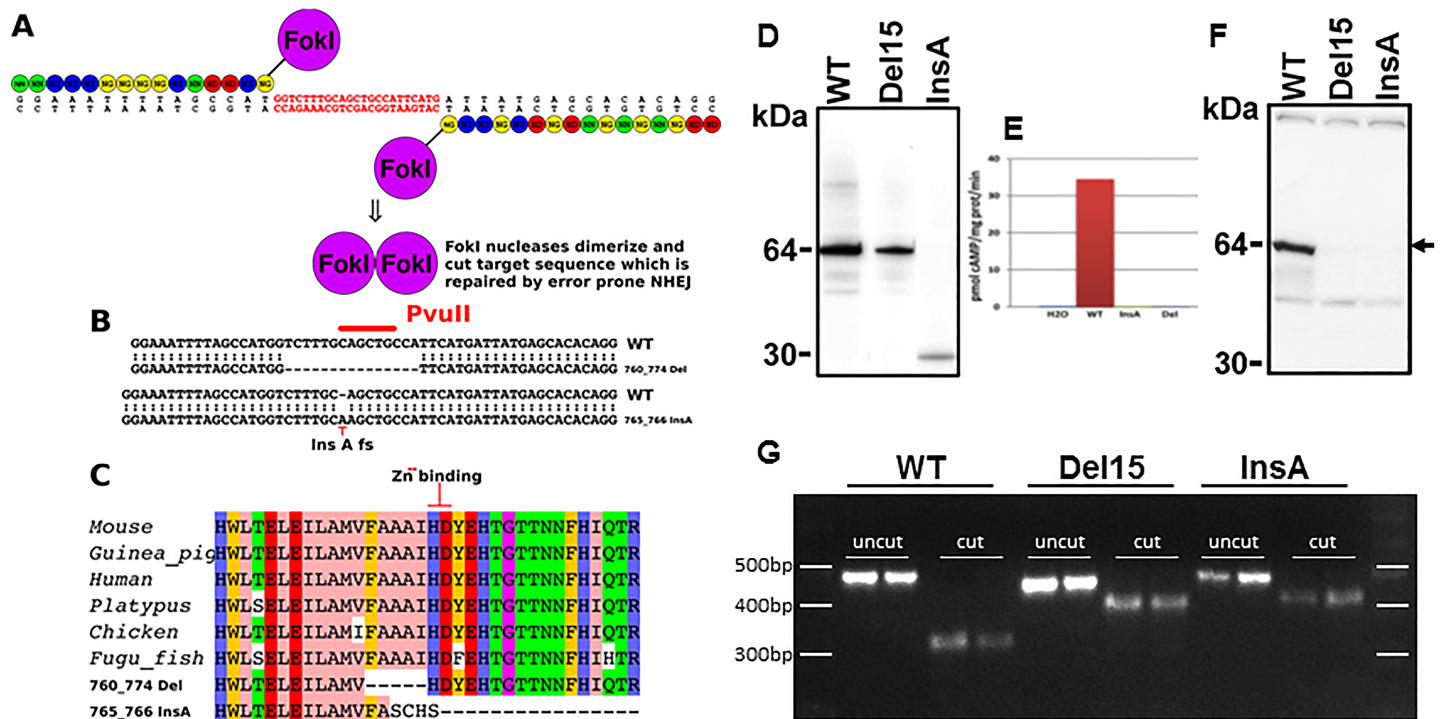


Fig 1. A) Left and right TALENs designed to disrupt exon 7 of mPde1a (active site). B) Recovered mutations include an in-frame 15bp deletion and insertion of a single A. C) Effect on mPde1a protein, the 15bp in frame deletion (760_774) removes amino acids FAAA and the insertion of an A (765_766) truncates mPde1a after four out of frame amino acids. D) Western blot of N-terminal V5-tagged wild-type and mutant mPde1a expressed in *Xenopus* oocytes detected with V5 antibody. E) PDE1 activity (Ca^{2+} /calmodulin dependent hydrolysis of cAMP) in *Xenopus* oocytes injected with water, wild-type RNA or mutated RNAs. F) Western blot of kidney lysates showing a 64 kDa protein in wild-type mice (arrow) detected with a rabbit polyclonal antibody raised against recombinant human PDE1A (360 C-terminal amino acids); this band was markedly reduced in *Pde1a*^{Del15} and absent in *Pde1a*^{InsA} homozygous mice. G) Reverse transcription of kidney RNA, PCR amplification and PvuII-HF restriction endonuclease digestion of a 485 bp PCR product, showing a 327 bp fragment in the wild-type and a 420 bp fragment in the mutants (smaller digest fragments are not resolved).

<https://doi.org/10.1371/journal.pone.0181087.g001>

Blood collections and tissue harvesting

Blood was obtained by cardiac puncture under ketamine (60mg/kg i.p.) and xylazine (10mg/kg i.p.) anesthesia. The right kidney and part of the liver were placed into preweighed vials containing 10% formaldehyde in phosphate buffer. The left kidney was immediately frozen in liquid nitrogen. Hearts were cut transversally and the apex was frozen immediately in liquid nitrogen while the rest was placed into vials containing 10% formaldehyde.

PDE activities

PDE activities in the kidneys and heart were measured as described in the Supplemental Material. Specific activities were expressed as picomoles of cAMP hydrolyzed per minute/mg of protein.

cAMP and cGMP content

The cAMP and cGMP were assessed by enzyme-linked immunosorbent assay (Enzo Life Sciences, Farmingdale, NY). Results were expressed in pmol/mg of protein.

Western blots

Immunoblotting of kidney and heart lysates or cytosol was performed as described in the Supplemental Material. Antibodies used were: PDE1A (12442-2-AP, Proteintech, Rosemount IL);

PDE1B (ab14600, Abcam, Cambridge, MA); PDE1C (sc67323, Santa Cruz, CA); pSer269--AQP2 (ab110418, Abcam, MA). The membrane was stained using swift membrane stain kit and total protein stain was used as loading control [14].

RT-PCR of tissue RNA

1 μ g of total RNA was reverse transcribed using SuperScript First-Strand Synthesis System (Invitrogen) in a total volume of 20 μ l at 37 $^{\circ}$ C for 1 hour. The PCR reactions were performed with 200nM mouse Pde1a specific primers: Forward: 5' -ATGCAGCTGACGTCCTCAAA, Reverse: 5' -AGGGCCATGGTCCATCTGTGA for 30 cycles at 95 $^{\circ}$ C for 40s, 60 $^{\circ}$ C for 1min and 72 $^{\circ}$ C for 1min. 10 μ l of the PCR products were digested with 10 μ l of a digest master mix using 0.3 μ l of PvuII-HF per reaction and digested overnight. The uncut PCR product is 484 bp. PvuII cut the PCR product to generate fragments of 327+93+58+6 bp in wild-type and 420+58+6 bp in *PDE1a*^{Del15} and *PDE1a*^{InsA}.

Histomorphometric and immunohistochemical analyses

These were performed as described in the Supplemental material. Antibodies used were against lysozyme (ab108508, Abcam, Cambridge, MA), Tamm-Horsfall protein (THP, sc20631, Santa Cruz, CA), aquaporin-2 (AQP2, sc9882, Santa Cruz, CA), epithelial membrane antigen (EMA, MA5-11202, Thermo Scientific, Rockford, IL), and proliferating cell nuclear antigen (PCNA, sc-56, Santa Cruz, CA).

Statistical analysis

Data are expressed as means \pm SD. One-way analysis of variance (ANOVA) with post-hoc Tukey test is used for comparisons between groups. The Student's *t*-test was used for comparisons between two groups.

Results

Pde1a mutants

Of eight pups carrying *Pde1a* mutations, we focused on an in frame deletion of 15bp, c.760-774del p.Phe254-Ile258del deleting amino acids FAAAI in the active site of mPDE1A (*Pde1a*^{Del15}) and an A insertion in the same region c.765-766insA p.Ala255fs5X which caused a frame shifting mutation that terminated the open reading frame after 4 out of frame amino acids (*Pde1a*^{InsA}) (Fig 1B and 1C). V5-tagged wild-type, *Pde1a*^{Del15} and *Pde1a*^{InsA} RNAs were injected into *Xenopus* oocytes. Western blotting with a V5 antibody showed a 64 kDa protein in the oocytes injected with the wild-type or *Pde1a*^{Del15} RNA and a truncated 30 kDa protein in oocytes injected with the *Pde1a*^{InsA} RNA (Fig 1D). In contrast to wild-type RNA, mutated RNAs failed to generate calcium/calmodulin dependent enzymatic activity when injected into *Xenopus* oocytes (Fig 1E). Western blot analysis of kidney lysates from wild-type mice with a PDE1A polyclonal antibody showed a 64 kDa protein, which was markedly reduced in *Pde1a*^{Del15} and absent in *Pde1a*^{InsA} mice (Fig 1F). Reverse transcription of kidney RNA, PCR amplification and PvuII-HF restriction endonuclease digestion of the 485 bp PCR product showed 6, 59, 93, and 327 bp fragments in the wild-type, 6, 59, and 420 bp fragments in the mutants, confirming the genotyping results (Fig 1G).

Characteristics of *Pde1a* knockout mice

The *Pde1a* alleles were produced on an inbred B57BL/6J background, identical to the background used to inbreed our PKD models. Male and female *Pde1a* mutant mice were fertile. Litter sizes, general appearance and pre-weaning or post-weaning growth of homozygous or

Table 1. Body and organ weights and laboratory parameters at 12 months of age.

	Wild-type (10 M, 9 F)	<i>Pde1a</i> ^{InsA/InsA} (9 M, 9 F)	<i>Pde1a</i> ^{Del15/Del15} (12 M, 19 F)	<i>Pde1a</i> ^{InsA/InsA or Del15/Del15} (21 M, 28 F)
Body weight, g	29.4±5.3	29.2±3.6	28.7±3.7	28.9±3.7
Kidney weight, g	0.42±0.08	0.45±0.06	0.47±0.09	0.46±0.08
Kidney weight, % BW	1.44±0.11	1.54±0.13*	1.63±0.26‡	1.60±0.22‡
Liver weight, g	1.48±0.31	1.32±0.23	1.40±0.30	1.37±0.28
Liver weight, % BW	5.03±0.57	4.56±0.79	4.88±0.72	4.76±0.76
Heart weight, g	0.18±0.05	0.20±0.03	0.20±0.04	0.20±0.12
Heart weight, % BW	0.63±0.10	0.68±0.12	0.69±0.11	0.69±0.12
Spleen weight, g	0.09±0.05	0.11±0.04	0.11±0.04	0.11±0.04
Spleen weight, % BW	0.34±0.13	0.39±0.19	0.38±0.14	0.38±0.16
Lung weight, g	0.22±0.04	0.23±0.04	0.25±0.04	0.24±0.04
Lung weight, % BW	0.78±0.18	0.81±0.20	0.88±0.18	0.86±0.19
Serum sodium, mEq/L	152.9±4.5	149.1±3.8	151.3±4.4	150.5±4.3
Serum potassium, mEq/L	7.1±0.9	7.0±1.1	7.3±1.1	7.2±1.1
Serum glucose, mg/dL	174±27	207±32	171±28	185±34
Serum creatinine, mg/dL	0.47±0.24	0.49±0.15	0.53±0.17	0.51±0.61

vs wild-type

*p<0.05

‡p<0.001.

BW: Body weight

<https://doi.org/10.1371/journal.pone.0181087.t001>

heterozygous *Pde1a*^{Del15} or *Pde1a*^{InsA} were not different from wild-type mice. At 12 months of age, kidney to body weight ratios were not different between *Pde1a*^{Del15/Del15} and *Pde1a*^{InsA/InsA} mice but both were significantly higher compared to the wild-type mice, whereas body weights, weights of other organs, and blood chemistries were similar (Table 1). Subsequently, both the homozygous *Pde1a*^{Del15} and *Pde1a*^{InsA} mice were considered as null models.

Activity and expression of PDE1, PDE3 and PDE4 families and cAMP levels in kidneys and hearts from *Pde1a*^{Del15} and *Pde1a*^{InsA} homozygotes compared to wild-type mice

In kidney tissue total PDE and PDE1 activities were reduced, whereas PDE3 and PDE4 activities were increased in both, *Pde1a*^{Del15/Del15} mice, as previously reported in younger animals [15], and in *Pde1a*^{InsA/InsA} mice compared to wild-type controls (Fig 2A). Total PDE, PDE1 and PDE3 activities were higher in the hearts than in the kidneys. In contrast to the kidneys, cardiac PDE1 activities were not lower and PDE3 and PDE4 activities were not higher in either model compared to wild-type mice. Expression of PDE1A protein was lower and expressions of PDE1B and PDE1C proteins were higher in hearts compared to kidneys of wild-type mice (Fig 2B). Renal cAMP levels tended to be higher in the kidneys but not in the hearts of *Pde1a* mutants compared to control animals (Fig 2C). Renal and cardiac cGMP levels in the *Pde1a* mutant and wild-type mice were not different (Fig 2C). PDE1A protein was expressed at higher levels in the aorta compared to the heart, with the highest level of expression being in the brain (Fig 2D).

Pde1a null mice developed mild renal cystic disease

At sacrifice the Kidney to body weight ratios of the *Pde1a*^{InsA/InsA} and *Pde1a*^{Del15/Del15} homozygous mice were higher than those of wild-type mice (Table 1, Fig 3A). MR scans of the

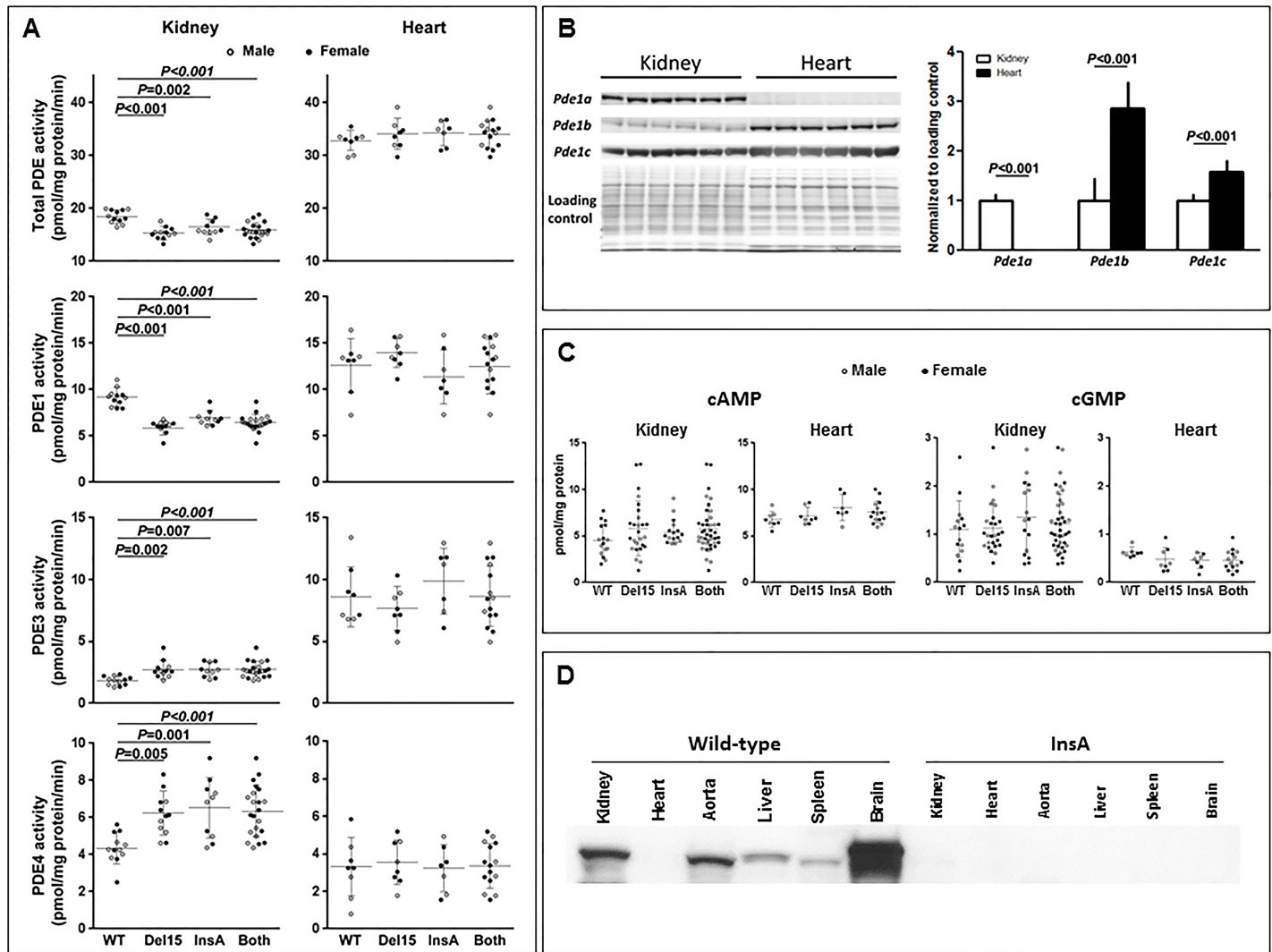


Fig 2. A) Total PDE, PDE1, PDE3 and PDE4 activities in kidney and heart lysates from wild-type mice and from *Pde1a*^{Del15} and *Pde1a*^{InsA} homozygous mice or results of both combined. B) Western blots of kidney and heart lysates from six wild-type mice detected with PDE1A, PDE1B and PDE1C antibodies; total protein stain with Coomassie Blue is used as a loading control. C) Cyclic AMP and cGMP levels in kidney and heart lysates from wild-type mice and from *Pde1a*^{Del15} and *Pde1a*^{InsA} homozygous mice or results of both combined. D) Western blot of kidney, heart, aorta, liver, spleen and brain lysates from wild-type and *Pde1a*^{InsA} homozygous mice detected with a PDE1A antibody; a weak cardiac band can be seen in wild-type with longer exposure (data not shown). One-way ANOVA with post-hoc Tukey test was used for the statistical analysis.

<https://doi.org/10.1371/journal.pone.0181087.g002>

kidneys were obtained at 6 and 12 months of age. At these ages small renal cysts were observed in 9 of 19 (47%, 8 *Pde1a*^{Del15/Del15} and 11 *Pde1a*^{InsA/InsA} mice) and 17 of 27 (63%, 20 *Pde1a*^{Del15/Del15} and 7 *Pde1a*^{InsA/InsA} mice) *Pde1a* mutant compared to 1 of 12 (13%, P = 0.046) and 1 of 10 (10%, P = 0.008) wild-type mice, respectively (Fig 3B and Fig B in S1 File). Histological examination of the kidneys at 12 months of age confirmed the presence of small cortical and medullary cysts and tubular dilatation in 26 of 44 (59%, 26 *Pde1a*^{Del15/Del15} and 18 *Pde1a*^{InsA/InsA} mice) *Pde1a* mutant compared to 3/18 (17%, P = 0.004) wild-type mice (P < 0.001). Only one or two small cysts confined to the inner medulla were observed in the three wild-type mice. MR and tissue sections showing small cysts in 12 month old wild-type mice are shown in Fig C in S1 File. Most dilated tubules and microscopic cysts stained positive with Tamm-Horsfall protein (THP, a marker for the thick ascending limb of Henle) and/or

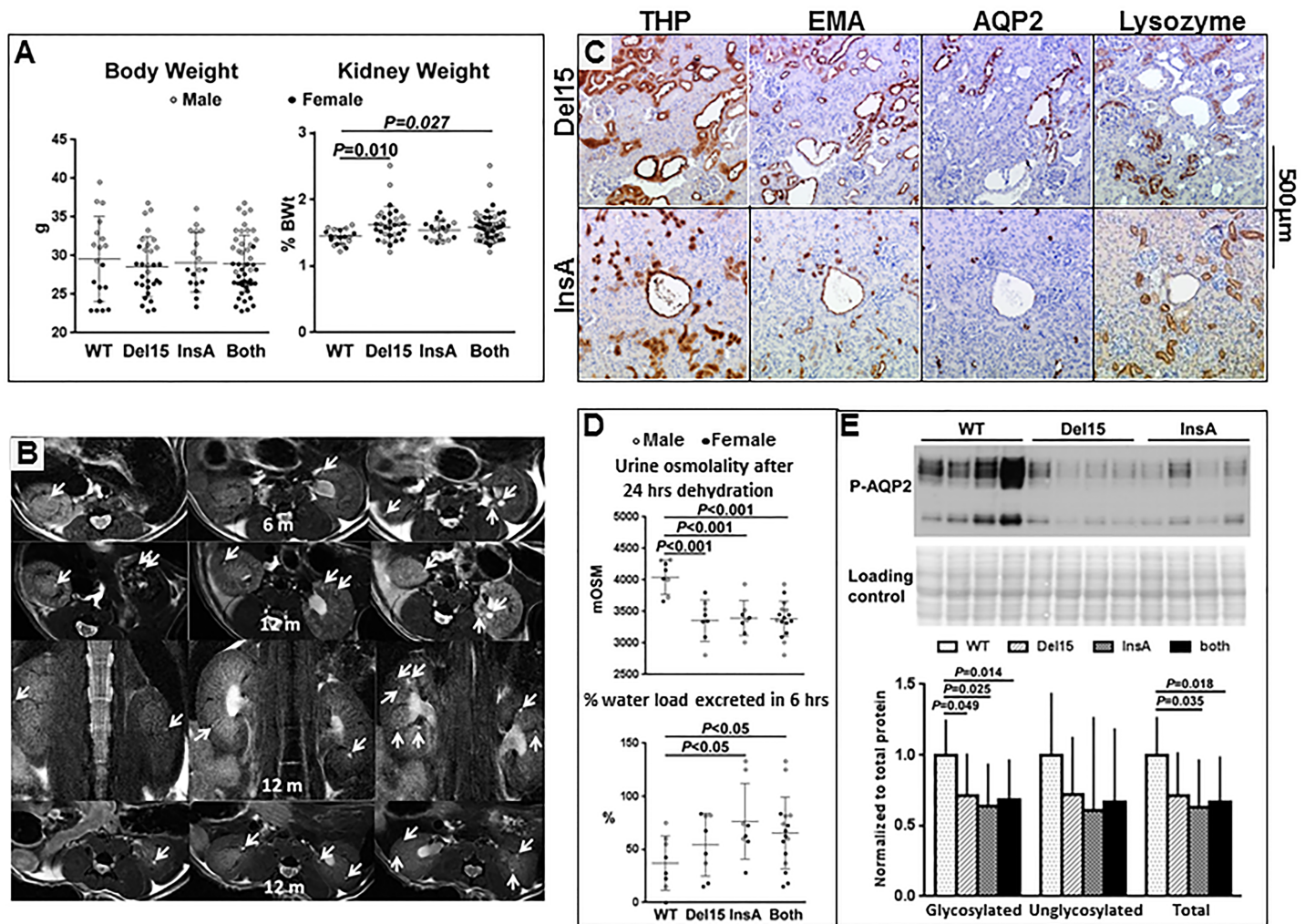


Fig 3. A) Body weight and kidney weight as percent of body weight (%KW/BW) in wild-type mice and in *Pde1a*^{Del15} and *Pde1a*^{InsA} homozygous mice or data from both combined. B) Axial and coronal MR images of *Pde1a* mutant mice at 6 and 12 months of age showing small renal cysts (arrows; this panel is also shown as a larger figure in Fig B in S1 File). C) Kidney sections from *Pde1a*^{Del15} and *Pde1a*^{InsA} homozygous mice showing multiple small cysts staining positively for Tamm-Horsfall protein and epithelial membrane antigen, less consistently for aquaporin-2, and not staining for lysozyme. D) Reduced urine osmolality after 24 hours of dehydration, faster excretion of an acute water load, and E) reduced expression of glycosylated (upper band) and unglycosylated (lower band) pSer269-AQP2 in *Pde1a*^{Del15} and *Pde1a*^{InsA} homozygotes compared to wild-type mice. One-way ANOVA with post-hoc Tukey test was used for the statistical analysis.

<https://doi.org/10.1371/journal.pone.0181087.g003>

epidermal membrane antigen (EMA, a marker for the distal nephron and collecting ducts), less often with aquaporin-2 (AQP-2, a marker for collecting duct principal cells), and were consistently negative for lysozyme (a proximal tubule marker; Fig 3C). Many cells in dilated tubules and microscopic cysts stained positive for PCNA (Fig 4).

Pde1a knockout mice had impaired urine concentrating capacity

The pool of cAMP generated in response to vasopressin is mainly hydrolyzed by PDE1 and the accumulation of cAMP in response to vasopressin is markedly increased when intracellular calcium is reduced, mainly due to lower PDE1 activity [16, 17]. We therefore anticipated that *Pde1a* knockout mice would have an enhanced urine concentrating capacity and impaired

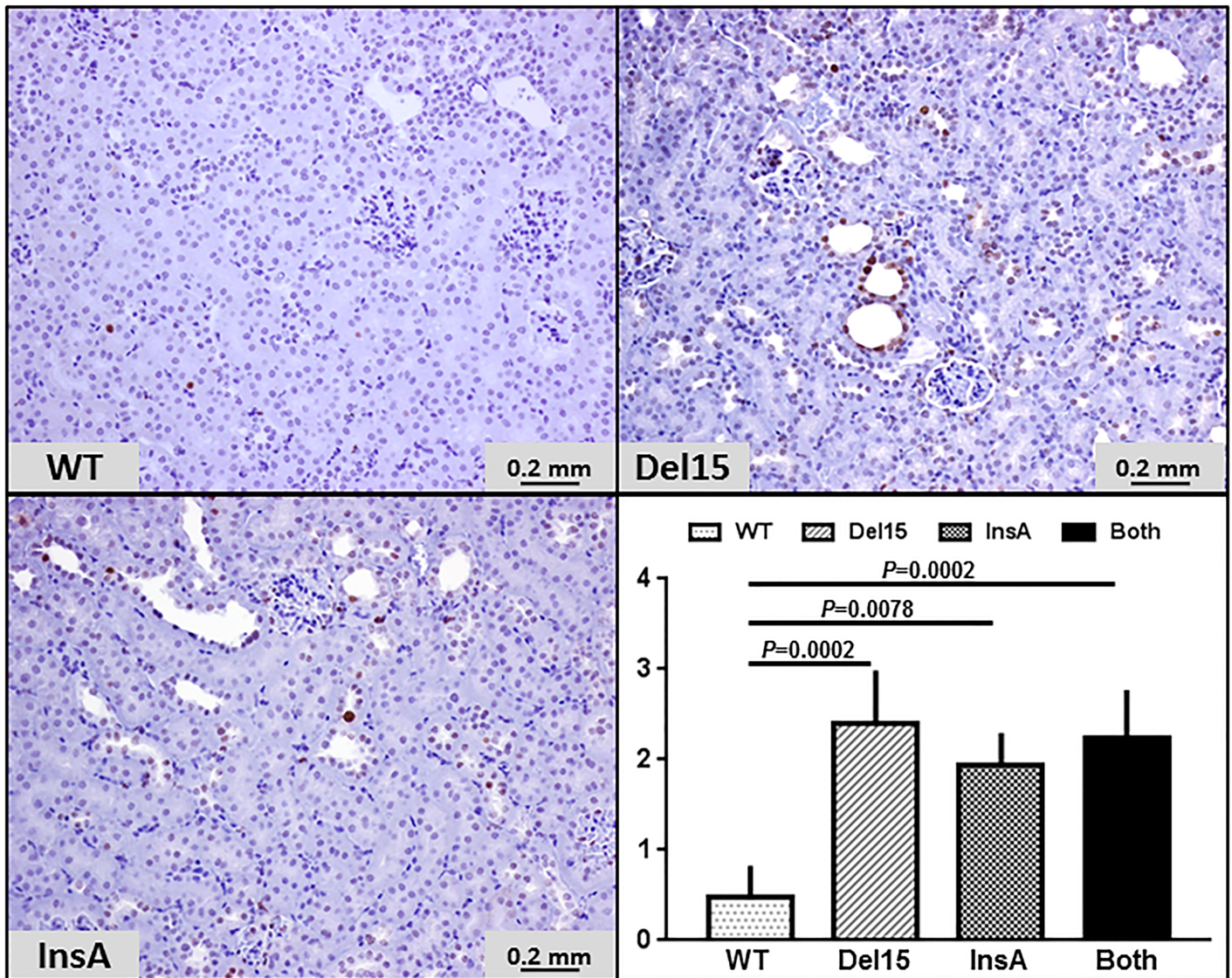


Fig 4. PCNA immunostaining of kidney sections (x 200) in wild-type mice (n = 4) and in *Pde1a*^{Del15} (n = 5) or *Pde1a*^{InsA} (n = 3) homozygous mice, and both combined (n = 8). Proliferative indices were significantly higher in the *Pde1a* mutants compared to the wild type mice. One-way ANOVA with post-hoc Tukey test was used for the statistical analysis.

<https://doi.org/10.1371/journal.pone.0181087.g004>

diluting capacity. Contrary to this expectation, we found that at 12 months of age these mice had a mild urine concentration defect after 24 hrs dehydration (3375 ± 312 and 3394 ± 273 compared to 4057 ± 255 mOsm/L in wild-type, $P < 0.01$, Fig 3D) and were able to excrete a water load faster (54 ± 29 and 77 ± 35 compared to $37 \pm 25\%$ of 2 ml ip over 6 hrs in wild-type mice, $P < 0.01$, Fig 3D). Since PDE4D controls a cAMP pool that regulates the expression, phosphorylation and translocation of AQP2 to the apical membrane of the collecting duct principal cells [18] and constitutive activation of PDE4 was found to be responsible for a mouse model of nephrogenic diabetes insipidus [19], we wondered whether the increased activity of PDE4 in the kidneys of the *Pde1a* mutants could be responsible for the mild concentration defect observed in these mice. Consistent with this, the expression of pSer269-AQP2 was decreased

in the kidneys of *Pde1a*^{Del15} and *Pde1a*^{InsA} homozygous mice compared to those of wild-type controls (Fig 3D).

Effect of desmopressin administration on the renal phenotype of *Pde1a*^{InsA/InsA} mice

The administration of desmopressin enhances the development of renal cystic disease in PCK rats and in *Pkd1*^{RC/RC} and *Pkd2*^{WS25/-} mice [8, 20]. To determine whether it could induce the development of renal cystic disease in *Pde1a* mutant mice, desmopressin (DDAVP, 30 ng/100 g BW/hr subcutaneously) or saline was administered to *Pde1a*^{InsA} homozygous and wild-type mice (5 male and 5 female mice per genotype and treatment) between 4 and 16 weeks of age. At 16 weeks of age the kidney to body weight ratios of desmopressin-treated *Pde1a* mutant mice were higher than those of saline-treated wild-type mice (Fig 5A). Two-way ANOVA showed that both *Pde1a* null genotype $P < 0.001$ and desmopressin treatment ($P = 0.004$) were associated with higher kidney to body weight ratios. Additionally, cAMP levels were higher in desmopressin-treated *Pde1a* mutant mice compared to control mutant and both wild-type groups. Prior to sacrifice, MRI of the kidneys were obtained in five *Pde1a*^{InsA} and four wild-type mice treated with desmopressin; three of the mutant and none of the wild-type mice had renal cysts (2–3 per animal, Fig 5A). Histological examination confirmed the presence of microscopic cysts staining positive for THP, EMA and less consistently AQP2 (Fig 5A).

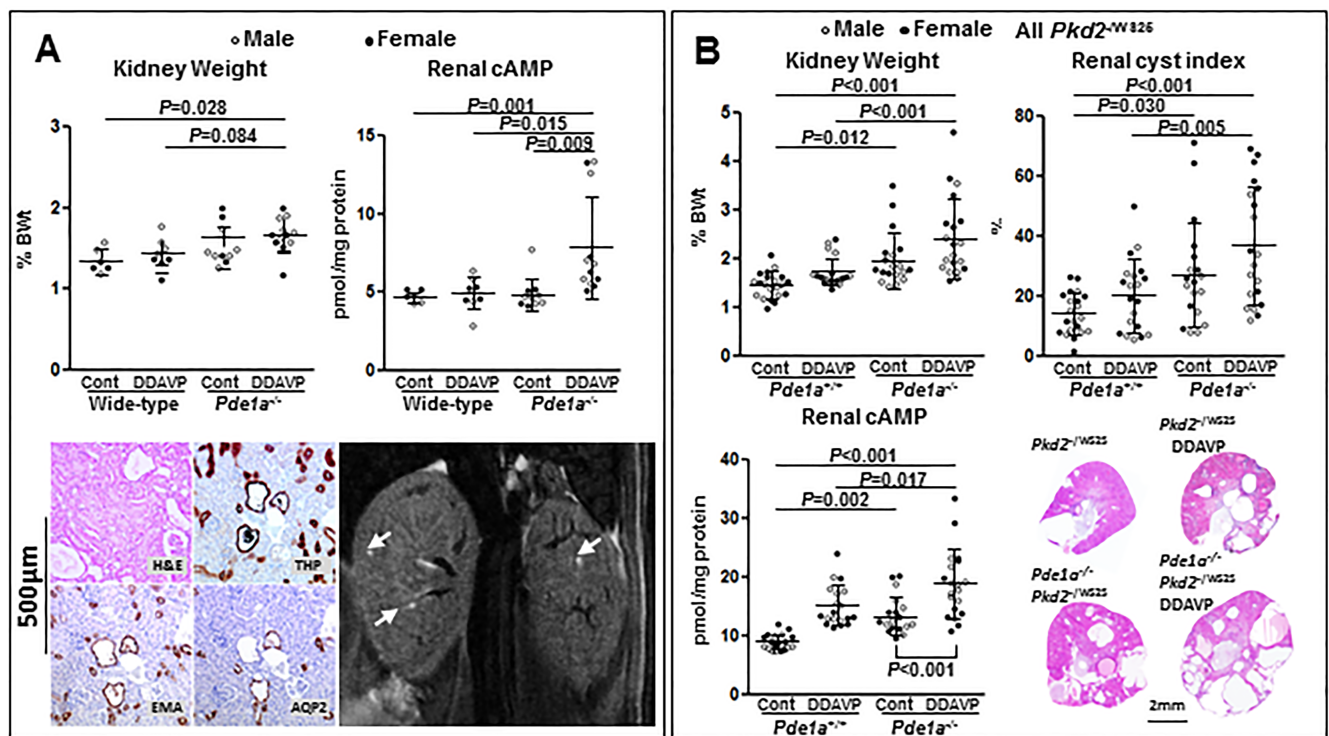


Fig 5. A) Upper panels: Kidney weights as percent of body weights (%KW/BW) and renal cAMP levels in untreated or desmopressin treated wild-type and *Pde1a*^{InsA} homozygous mice (upper panels); One-way ANOVA with post-hoc Tukey test was used for the statistical analysis; using a two-way ANOVA, both *Pde1a* null genotype $P < 0.001$ and desmopressin treatment ($P = 0.004$) were associated with higher kidney to body weight ratios. Lower panels: Kidney sections stained with hematoxylin-eosin or immunostained with Tamm-Horsfall protein, epithelial membrane antigen or aquaporin-2 antibodies, and coronal MR image showing small cysts (arrows) in desmopressin treated *Pde1a*^{InsA} homozygous mice. B) %KW/BW, kidney cystic indices, renal cAMP levels, and kidney sections stained with hematoxylin-eosin in untreated or desmopressin treated *Pkd2*^{WS25} and *Pkd2*^{WS25}, *Pde1a*^{Del15/Del15} mice. One-way ANOVA with post-hoc Tukey test was used for the statistical analysis.

<https://doi.org/10.1371/journal.pone.0181087.g005>

The development of polycystic kidney disease in *Pkd2*^{/WS25} mice was enhanced on a *Pde1a* null genetic background and aggravated by the administration of desmopressin

We previously reported that the development of PKD in *Pkd2*^{/WS25} mice is aggravated on a *Pde1a* or a *Pde3a* null background [15]. We also suggested that the lower susceptibility to PKD and enhanced disease associated with desmopressin treatment, when comparing mice to rats, may be due to higher PDE activities in mouse compared to rat kidneys [20, 21]. Indeed we found that administration of desmopressin aggravated the renal cystic disease of *Pkd2*^{/WS25} mice on a *Pde3a* null background compared desmopressin-treated *Pkd2*^{/WS25} mice on a wild-type background [15]. To determine whether the cystogenic effects of desmopressin would also be enhanced on a *Pde1a* null background, we administered desmopressin (30 ng/100 g BW per hour subcutaneously) or saline to *Pkd2*^{/WS25}; *Pde1a*^{Del15/Del15} and *Pkd2*^{/WS25} mice. Kidney to body weight ratios and cystic indices were significantly higher in desmopressin-treated *Pkd2*^{/WS25} mice on a *Pde1a* null background compared to saline- or desmopressin-treated *Pkd2*^{/WS25} mice on a wild-type background (Fig 5B). Kidney to body weight ratios and cystic indices were numerically higher in desmopressin-treated compared to saline-treated *Pkd2*^{/WS25} mice on a *Pde1a* null background, without reaching statistical significance ($P = 0.054$ and 0.20 , respectively).

Pde1a knockout mice have a cardiovascular phenotype

Because of the association of various cardiac phenotypes with PKD [22, 23] and the finding that PDE1 accounts for a major component of PDE activity in the heart, we tested whether inactivation of *Pde1a* results in a cardiac or cardiovascular phenotype. We found that both *Pde1a*^{Del15} and *Pde1a*^{InsA} mice had lower aortic blood pressures (Fig 6A) and higher LV ejection fractions on echocardiography (Fig 6B) compared to wild-type mice. However, there was no difference in LV mass index measured by MRI between *Pde1a* wild-type and mutant mice (Fig 6C).

Discussion

A substantial body of evidence indicates that cAMP and PKA signaling play a central role in PKD [3–5]. It has been proposed that a reduction in intracellular calcium causes the upregulation of cAMP and PKA through stimulation of calcium-inhibitable adenylyl cyclase 6 and inhibition of PDE1, the main enzymes generating and degrading cAMP in the distal nephron and collecting duct [6]. Consistent with this hypothesis, a collecting duct-specific knockout of adenylyl cyclase 6 affords protection in a *Pkd1* mouse model [24]. Since capacity for hydrolysis of cyclic nucleotides by PDEs far exceeds that for synthesis by adenylyl cyclases [25], modulation of PDE activity, particularly PDE1 activity, may be crucial in PKD.

PDE1 is one of eleven mammalian PDE families (PDE1–PDE11) with twenty-two genes and close to 100 distinct isoenzyme variants generated through the use of alternate promoter initiation sites and/or alternate splicing [26, 27]. PDE family members may exclusively hydrolyze cAMP or cGMP, or they may hydrolyze both. PDE activities are regulated by phosphorylation/dephosphorylation (e.g. PDE4 activation by PKA phosphorylation), binding of cGMP (e.g. PDE3 inhibition by cGMP) or cAMP, binding of calcium/calmodulin (PDE1 activation by calcium/calmodulin), and various protein-protein interactions. Differences in the subcellular localization of the different PDEs are important for the functional compartmentalization of cAMP-mediated responses [28].

The interest in PDE1 in the pathogenesis of PKD arose from the facts that PC2 is a TRP channel with permeability to calcium and that PDE1 is the only PDE family directly regulated

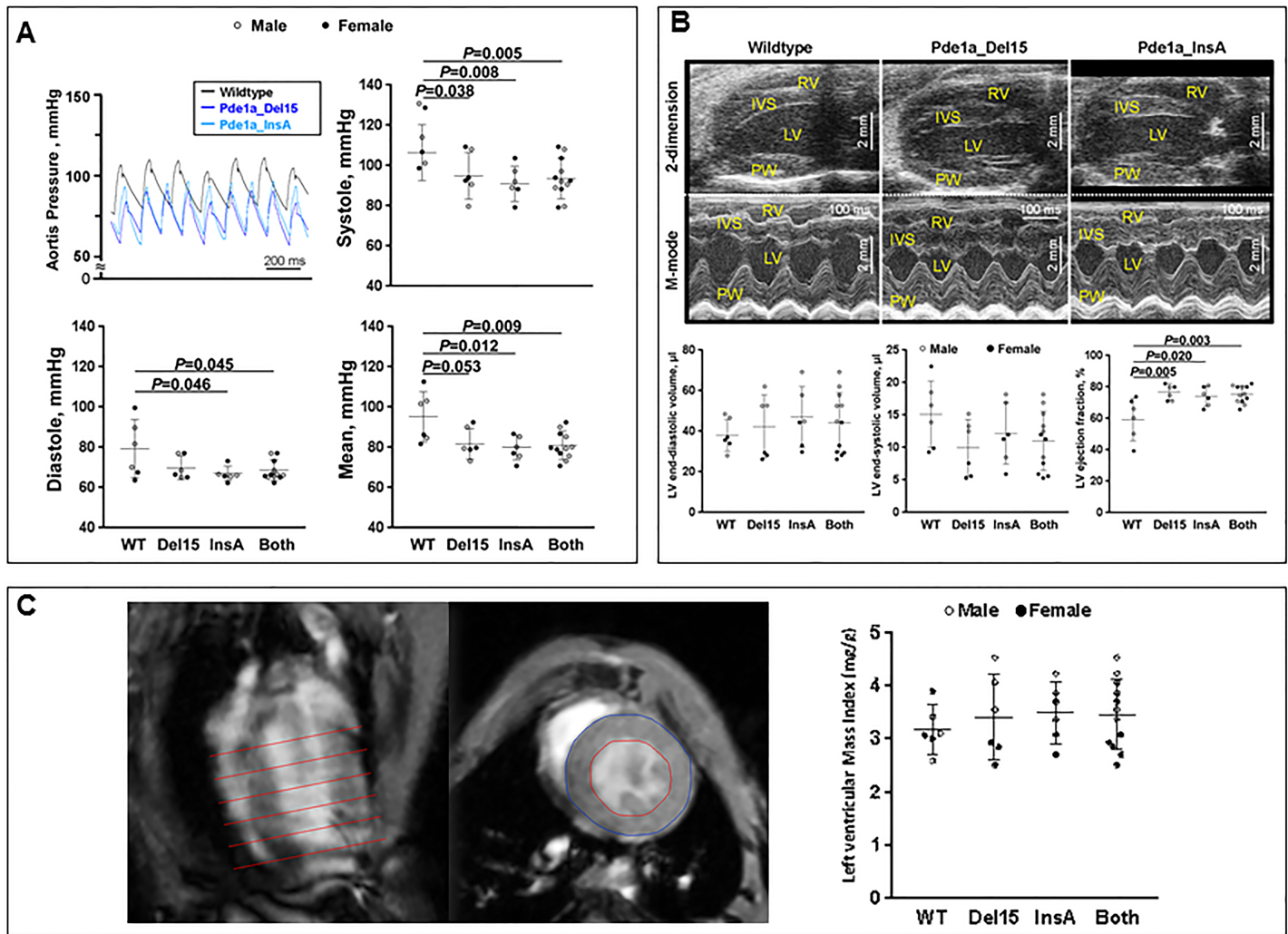


Fig 6. A) Aortic blood pressures were lower in *Pde1a*^{Del15} and *Pde1a*^{InsA} homozygous mice compared to wild-type mice. B) Echocardiographic studies showing increased LV ejection fractions in *Pde1a*^{Del15} and *Pde1a*^{InsA} homozygous mice compared to wild-types; RV: Right ventricle; LV: Left ventricle; IVS: Interventricular septum; PW: Posterior wall C) Measurements of LV mass index using MRI show no significant difference between wild-type and *Pde1a* mutant mice. One-way ANOVA with post-hoc Tukey test was used for the statistical analysis.

<https://doi.org/10.1371/journal.pone.0181087.g006>

by calcium and calmodulin [29–32]. The PDE1 family consists of three members encoded by three different genes. PDE1A and PDE1B have a higher affinity for cGMP than for cAMP, while PDE1C is equally active for both. PDE1s integrate intracellular calcium levels and cAMP and cGMP signaling. Phosphorylation of PDE1A and PDE1C by PKA and of PDE1B by calcium/calmodulin-dependent protein kinase II reduces their activity via reduced affinity for calmodulin and sensitivity to calcium. PDE1 isoforms are dephosphorylated and reactivated by calcium/calmodulin-dependent protein phosphatase (calcineurin; protein phosphatase 2B).

PDE1 is the most abundant PDE in the distal nephron and collecting duct [33] and catabolizes a cAMP pool under the control of vasopressin and the vasopressin V2 receptor [16, 34]. Therefore we expected that the knockout of *Pde1a* would result in accumulation of cAMP, increased PKA-dependent phosphorylation and trafficking of AQP2 to the apical membrane of collecting duct principal cells, and enhanced urine concentrating capacity. Unexpectedly, however, we found that the *Pde1a* deficient mice were less able to concentrate the urine

maximally and more capable to excrete an acute water load compared to wild-type controls. In retrospect, this could have been anticipated because phosphorylation and shuttling of AQP-2 to the plasma membrane and water permeability in the principal cells of collecting ducts is under the control of a compartmentalized pool of PDE4D bound to AKAP18delta in aquaporin-2 bearing vesicles [18]. Since PDE4 is activated by PKA-mediated phosphorylation, downregulation of PDE1 and subsequent activation of PKA may account for the increased PDE4 activity, reduced PKA-dependent phosphorylation of AQP-2, and concentrating defect observed in our study.

Interest in the role of cAMP and its interaction with calcium as regulators of cell proliferation dates back almost to its identification as the first known second intracellular messenger [35]. Remarkably, cAMP inhibits cell proliferation in some cells (e.g. vascular smooth muscle cells, mesangial cells, endothelial cells, fibroblasts, adipocytes, hepatocytes) while having the opposite effect in others (thyrocytes, pituitary cells, PC12 pheochromocytoma cells, granulosa cells, Sertoli cells, neurons, melanocytes) [36, 37]. The mechanisms by which cAMP modulates cell proliferation are complex, poorly understood and involve interactions with the RAS/RAF/mitogen-activated protein kinase (MAPK) and extracellular signal-regulated kinase (ERK) kinase (MEK)/ERK pathway at multiple levels [36, 37]. Cyclic AMP can stimulate or inhibit cell proliferation via activation or inhibition of ERK, respectively, as well as independently of this pathway, in a cell and context dependent manner. The type of response depends on the strength and duration of signaling, the subcellular localization of involved adenylyl cyclases, A-kinase anchoring proteins, PKA regulatory subunits, phosphodiesterases, and exchange proteins activated by cAMP (Epacs), and the relative expressions of Rap-1, B-Raf versus Raf-1, and B-Raf isoforms, among others.

Previous studies have shown that cAMP stimulates proliferation of PKD-derived tubular epithelial cells while inhibiting proliferation of wild-type tubular epithelial cells [38–40]. These contrasting effects of cAMP are likely determined by the level of intracellular calcium, since the cAMP induced proliferation of ADPKD cells is reversed by activators of L-type calcium channels or by calcium ionophores. Similarly, the response of wild-type tubular epithelial cells to cAMP can be switched from inhibition to stimulation of proliferation by lowering free extracellular calcium or by calcium channel blockers. Inhibition of calcium dependent PI3K and Akt, which under normal calcium conditions phosphorylate and repress B-Raf, has been proposed to account for the proliferative effect of cAMP under conditions of calcium restriction.

The subcellular localization of the different PDEs is crucial for the functional compartmentalization of cAMP-mediated responses, and likely explains the lack of significant effect on total tissue cAMP and cGMP levels detected in PDE1A mutants despite a difference in PDE1 activity. Inhibitory and stimulatory effects of cAMP on cell proliferation have both been linked to a cAMP pool regulated by PDE3. In mesangial cells, PDE3 and PDE4 inhibitors increase cAMP levels and activate PKA to a similar extent, but only PDE3 inhibitors block phosphorylation of Raf-1 on serine 338, suppress Raf-1 kinase activity and ERK activation, and regulate proliferation [41, 42]. PDE3, but not PDE4 inhibitors, impede the proliferation of vascular smooth muscle and endothelial cells [43]. Despite the fact that PDE4 is three times more active than PDE3 in suspensions of renal cortical tubules, only PDE3 inhibitors suppress the proliferation of wild-type tubular epithelial cells following administration of folic acid [44]. On the other hand, only PDE3 inhibitors stimulate proliferation of MDCK cells (often used for cAMP inducible *in vitro* cystogenesis) despite the fact that PDE4 inhibitors are more effective in elevating intracellular cAMP levels in these cells [45].

The role of PDE1 in the control of cell proliferation has received less attention. In VSMCs, PDE1 inhibition or RNA interference of either PDE1A or PDE1C suppresses cell proliferation

[46–48]. Since inhibition of PDE1 is expected to increase cGMP and cGMP inhibits PDE3, it is possible that downregulation of PDE1 indirectly affects a specific pool of intracellular cAMP under the control of PDE3. Interestingly, depletion of either, PDE1A or PDE3A using morpholinos causes pronephric cysts, body curvature, and hydrocephalus in zebrafish [12, 49]. A recent study has shown that inhibition of PDE1 or PDE3 stimulates the proliferation of ADPKD cells and that inhibition of PDE1 induces a mitogenic response to vasopressin in normal human kidney cells similar to the effect of restricting intracellular calcium [50]. These observations raise the possibility that PDE1 may function as a link connecting changes in intracellular calcium and the activity of a PDE3 pool controlling cell proliferation. The mild cystic disease observed in the present study affected the distal nephron (mainly the thick ascending limb of Henle) and collecting ducts, consistent with the pattern of expression of vasopressin V2 receptor [51, 52]. The knockout of *Pde1a* resulted only in a moderate reduction in PDE1 activity, likely due to redundancy with other PDE1 subfamilies, PDE1C and PDE1B.

We investigated whether *Pde1a* knockout mice had a cardiac phenotype for several reasons: i) Cardiovascular manifestations (hypertension, LV hypertrophy, cardiac valvular disease, cardiomyopathies, aortic root dilatation, arterial aneurysms and dissections, and pericardial effusion) are common causes of morbidity and mortality in ADPKD [22, 23]; ii) PDE1A has been proposed to play a role in the development of cardiac hypertrophy; iii) The polycystins are expressed in cardiac and arterial myocytes [53–56]; and iv) Knockdowns of either polycystin in mice and of PC2 in zebrafish impair myocardial function in the absence of renal cysts [57–60].

PDE1 is one of at least seven PDE families (PDE1 to PDE5, PDE8 and PDE9) present in mammalian hearts [61]. Reports on its importance relative to other PDE families and the relative expression of the three PDE1 subfamilies in different animal species have not been consistent (Table A in S1 File)[62–74]. Overall, our findings agree with some but not all published studies: i) PDE1 accounts for a large proportion of cAMP-PDE activity in the heart [65–67, 70]; ii) The protein expression of PDE1C is much higher than that of PDE1A in the myocardium [63, 64, 67, 72–74]; iii) Therefore, PDE1C is likely more important for cardiac hypertrophy than PDE1A; iv) The protein expression of PDE1A is much higher in adult aorta [32, 47, 75]; v) Consistent with this pattern of expression, *Pde1a* knockout mice in our study had lower blood pressures and a hyperdynamic circulation with an increased heart rate and ejection fraction. Interestingly, a large gene-centric meta-analysis in 87,736 individuals of European ancestry has identified an association between the *PDE1A* locus and diastolic and mean arterial pressures [76], and mutations of *PDE3A* resulting in increased PKA-mediated PDE3A phosphorylation and gain of function have been found in six families with hypertension and brachydactily syndrome [77]. On the other hand, PDE1 and PDE3 degrade cAMP in the juxtaglomerular cells thus inhibiting the release of renin and lowering blood pressure [78, 79].

While these observations do not support a role for a deficiency of PDE1A in the cardiac manifestations of ADPKD, a role for a defect in PDE1A, another PDE1 subfamily or another PDE family is still possible. In particular, it should be kept in mind that the consequences of inhibiting PDE1 on PDE3 activity may be different in a wild-type versus a PKD genetic background. While PDE1A is expressed at low level if at all in cardiac myocytes, it is highly expressed in the cardiac sinoatrial nodal cells where it regulates pacemaker function. Possibly, dysregulation of PDE1A activity could contribute to the increased prevalence of atrial fibrillation reported in ADPKD [80]. While PDE1C and PDE3A inhibitors attenuate cardiac hypertrophy and PDE3 inhibitors in the short term enhance LV contractility and overall systolic function, prolonged inhibition of PDE3 is detrimental because it promotes apoptosis and hypertrophy of the remaining cardiac myocytes [81].

In summary, PDE1A is strongly expressed in the kidney and the aorta. Knocking out *Pde1a* induced mild renal cystic disease and a urine concentrating defect (associated with

upregulation of PDE4 activity and a decrease in protein kinase A dependent phosphorylation of aquaporin-2) on a wild-type genetic background and aggravated the renal cystic disease on a *Pkd2*^{WS25/-} background. *Pkd1a* mutants had lower aortic blood pressure and increased LV ejection fraction without a change in LV mass index, consistent with the high aortic and low cardiac expression of *Pde1a* in wild-type mice. These results support an important role of PDE1A in the renal pathogenesis of ADPKD and regulation of blood pressure.

Supporting information

S1 File. Fig A. Genomic DNA PCR amplification and PvuII-HF restriction endonuclease digestion of a 792 bp PCR product, showing a 669 and 123 bp fragments in the wild-type, a 777 bp fragment in Del15 and a 793 bp fragment in Insa (A, upper panel). With a longer run to better separate the upper bands, the lower 123bp band disappears (B, lower panel). **Fig B.** Axial and coronal MR images of *Pde1a* mutant mice at 6 and 12 months of age showing small renal cysts (arrows). **Fig C.** Small cysts demonstrated by MRI in a 12 month-old, male wild type mouse (A) and by histology in 12 month old, female wild-type mouse (B) (DOCX)

Acknowledgments

This work was supported by grants from the National Institutes of Health (DK44863 and DK90728) and by the Mayo Clinic Robert M. and Billie Kelley Pirnie Translational PKD Research Center.

Author Contributions

Conceptualization: Fouad T. Chebib, Peter C. Harris, Caroline R. Sussman, Vicente E. Torres.

Data curation: Xiaofang Wang, Satsuki Yamada, Jason L. Bakeberg.

Formal analysis: Xiaofang Wang, Satsuki Yamada.

Funding acquisition: Peter C. Harris, Christopher J. Ward, Vicente E. Torres.

Investigation: Xiaofang Wang, Wells B. LaRiviere, Hong Ye, Jason L. Bakeberg, Jan van Deursen, Atta Behfar, Christopher J. Ward.

Methodology: Xiaofang Wang, Jason L. Bakeberg, María V. Irazabal, Jan van Deursen, Christopher J. Ward, Vicente E. Torres.

Project administration: Xiaofang Wang, Vicente E. Torres.

Resources: Jan van Deursen, Vicente E. Torres.

Supervision: Christopher J. Ward, Vicente E. Torres.

Validation: Xiaofang Wang, Vicente E. Torres.

Visualization: Xiaofang Wang.

Writing – original draft: Xiaofang Wang, Vicente E. Torres.

Writing – review & editing: Xiaofang Wang, Satsuki Yamada, Wells B. LaRiviere, Hong Ye, Jason L. Bakeberg, María V. Irazabal, Fouad T. Chebib, Jan van Deursen, Peter C. Harris, Caroline R. Sussman, Atta Behfar, Christopher J. Ward, Vicente E. Torres.

References

1. Ong AC, Devuyst O, Knebelmann B, Walz G, Diseases E-EWGfIK. Autosomal dominant polycystic kidney disease: the changing face of clinical management. *Lancet*. 2015; 385(9981):1993–2002. [https://doi.org/10.1016/S0140-6736\(15\)60907-2](https://doi.org/10.1016/S0140-6736(15)60907-2) PMID: 26090645
2. Chapman AB, Devuyst O, Eckardt KU, Gansevoort R, Harris TB, Horie S, et al. Autosomal dominant polycystic kidney disease (ADPKD): executive summary from a Kidney Disease: Improving Global Outcomes (KDIGO) Controversies Conference. *Kidney Int*. 2015; 88(1):17–27. <https://doi.org/10.1038/ki.2015.59> PMID: 25786098
3. Torres VE, Harris PC. Strategies targeting cAMP signaling in the treatment of polycystic kidney disease. *J Am Soc Nephrol*. 2014; 25(1):18–32. <https://doi.org/10.1681/ASN.2013040398> PMID: 24335972
4. Calvet JP. The Role of Calcium and Cyclic AMP in PKD. In: Li X, editor. *Polycystic Kidney Disease*. Brisbane (AU)2015.
5. Chebib FT, Sussman CR, Wang X, Harris PC, Torres VE. Vasopressin and disruption of calcium signaling in polycystic kidney disease. *Nat Rev Nephrol*. 2015(8):451–64. <https://doi.org/10.1038/nrneph.2015.39> PMID: 25870007
6. Gattone VH, Wang X, Harris PC, Torres VE. Inhibition of renal cystic disease development and progression by a vasopressin V2 receptor antagonist. *Nature Med*. 2003; 9:1323–6. <https://doi.org/10.1038/nm935> PMID: 14502283
7. Torres VE, Wang X, Qian Q, Somlo S, Harris PC, Gattone VH. Effective treatment of an orthologous model of autosomal dominant polycystic kidney disease. *Nature Med*. 2004; 10:363–4. <https://doi.org/10.1038/nm1004> PMID: 14991049
8. Wang X, Wu Y, Ward CJ, Harris PC, Torres VE. Vasopressin directly regulates cyst growth in polycystic kidney disease. *J Am Soc Nephrol*. 2008; 19(1):102–8. <https://doi.org/10.1681/ASN.2007060688> PMID: 18032793
9. Reif GA, Yamaguchi T, Nivens E, Fujiki H, Pinto CS, Wallace DP. Tolvaptan inhibits ERK-dependent cell proliferation, Cl(-) secretion, and in vitro cyst growth of human ADPKD cells stimulated by vasopressin. *Am J Physiol Renal Physiol*. 2011; 301(5):F1005–13. <https://doi.org/10.1152/ajprenal.00243.2011> PMID: 21816754
10. Torres VE, Chapman AB, Devuyst O, Gansevoort RT, Grantham JJ, Higashihara E, et al. Tolvaptan in Patients with Autosomal Dominant Polycystic Kidney Disease. *N Engl J Med*. 2012; 367(25):2407–18. <https://doi.org/10.1056/NEJMoa1205511> PMID: 23121377
11. Caroli A, Perico N, Perna A, Antiga L, Brambilla P, Pisani A, et al. Effect of long acting somatostatin analogue on kidney and cyst growth in autosomal dominant polycystic kidney disease (ALADIN): a randomised, placebo-controlled, multicentre trial. *Lancet*. 2013; 382(9903):1485–95. [https://doi.org/10.1016/S0140-6736\(13\)61407-5](https://doi.org/10.1016/S0140-6736(13)61407-5) PMID: 23972263
12. Sussman CR, Ward CJ, Leightner AC, Smith JL, Agarwal R, Harris PC, et al. Phosphodiesterase 1A Modulates Cystogenesis in Zebrafish. *J Am Soc Nephrol*. 2014; 25(10):2222–30. <https://doi.org/10.1681/ASN.2013040421> PMID: 24700876
13. Card GL, England BP, Suzuki Y, Fong D, Powell B, Lee B, et al. Structural basis for the activity of drugs that inhibit phosphodiesterases. *Structure*. 2004; 12(12):2233–47. <https://doi.org/10.1016/j.str.2004.10.004> PMID: 15576036
14. Aldridge GM, Podrebarac DM, Greenough WT, Weiler IJ. The use of total protein stains as loading controls: an alternative to high-abundance single-protein controls in semi-quantitative immunoblotting. *J Neurosci Methods*. 2008; 172(2):250–4. <https://doi.org/10.1016/j.jneumeth.2008.05.003> PMID: 18571732
15. Ye H, Wang X, Sussman CR, Irazabal MV, Vorhees CV, Zhao H, et al. Modulation of Polycystic Kidney Disease Severity by PDE1 and PDE3 Subfamilies. *J Am Soc Nephrol*. 2016; 27(5):1312–20. <https://doi.org/10.1681/ASN.2015010057> PMID: 26374610
16. Yamaki M, McIntyre S, Rassier ME, Schwartz JH, Dousa TP. Cyclic 3',5'-nucleotide diesterases in dynamics of cAMP and cGMP in rat collecting duct cells. *Am J Physiol*. 1992; 262(6 Pt 2):F957–64.
17. Kusano E, Murayama N, Werness JL, Christensen S, Homma S, Yusufi AN, et al. Effects of calcium on the vasopressin-sensitive cAMP metabolism in medullary tubules. *Am J Physiol*. 1985; 249(6 Pt 2): F956–66.
18. Stefan E, Wiesner B, Baillie GS, Mollajew R, Henn V, Lorenz D, et al. Compartmentalization of cAMP-dependent signaling by phosphodiesterase-4D is involved in the regulation of vasopressin-mediated water reabsorption in renal principal cells. *J Am Soc Nephrol*. 2007; 18(1):199–212. <https://doi.org/10.1681/ASN.2006020132> PMID: 17135396
19. Takeda S, Lin CT, Morgano PG, McIntyre SJ, Dousa TP. High activity of low-Michaelis-Menten constant 3', 5'-cyclic adenosine monophosphate-phosphodiesterase isozymes in renal inner medulla of mice

- with hereditary nephrogenic diabetes insipidus. *Endocrinology*. 1991; 129(1):287–94. <https://doi.org/10.1210/endo-129-1-287> PMID: 1647298
20. Hopp K, Wang X, Ye H, Irazabal MV, Harris PC, Torres VE. Effects of hydration in rats and mice with polycystic kidney disease. *Am J Physiol*. 2015; in press.
 21. Wang X, Ward CJ, Harris PC, Torres VE. Cyclic nucleotide signaling in polycystic kidney disease. *Kidney Int*. 2010; 77(2):129–40. <https://doi.org/10.1038/ki.2009.438> PMID: 19924104
 22. Ecker T. Cardiovascular complications in autosomal dominant polycystic kidney disease. *Curr Hypertens Rev*. 2013; 9(1):2–11. PMID: 23971638
 23. Chebib FT, Hogan MC, El-Zoghby Z, Irazabal Mira MV, Senum SR, Heyer CM, et al. Autosomal Dominant Polycystic Kidney Patients May Be Predisposed to Various Cardiomyopathies. SUBMITTED. 2017.
 24. Rees S, Kittikuluth W, Roos K, Strait KA, Van Hoek A, Kohan DE. Adenylyl cyclase 6 deficiency ameliorates polycystic kidney disease. *J Am Soc Nephrol*. 2014; 25(2):232–7. <https://doi.org/10.1681/ASN.2013010077> PMID: 24158982
 25. Dousa TP. Cyclic-3',5'-nucleotide phosphodiesterase isozymes in cell biology and pathophysiology of the kidney. *Kidney Int*. 1999; 55(1):29–62. <https://doi.org/10.1046/j.1523-1755.1999.00233.x> PMID: 9893113
 26. Bender AT, Beavo JA. Cyclic nucleotide phosphodiesterases: molecular regulation to clinical use. *Pharmacol Rev*. 2006; 58(3):488–520. <https://doi.org/10.1124/pr.58.3.5> PMID: 16968949
 27. Ahmad F, Degerman E, Manganiello VC. Cyclic nucleotide phosphodiesterase 3 signaling complexes. Hormone and metabolic research = Hormon- und Stoffwechselforschung = Hormones et métabolisme. 2012; 44(10):776–85. <https://doi.org/10.1055/s-0032-1312646> PMID: 22692928
 28. Brescia M, Zaccolo M. Modulation of Compartmentalised Cyclic Nucleotide Signalling via Local Inhibition of Phosphodiesterase Activity. *Int J Mol Sci*. 2016; 17(10).
 29. Goraya TA, Cooper DM. Ca²⁺-calmodulin-dependent phosphodiesterase (PDE1): current perspectives. *Cell Sig*. 2005; 17(7):789–97.
 30. Sharma RK, Das SB, Lakshmikuttyamma A, Selvakumar P, Shrivastav A. Regulation of calmodulin-stimulated cyclic nucleotide phosphodiesterase (PDE1): review. *Int J Mol Med*. 2006; 18(1):95–105. PMID: 16786160
 31. Kakkar R, Raju RV, Sharma RK. Calmodulin-dependent cyclic nucleotide phosphodiesterase (PDE1). *Cell Mol Life Sci*. 1999; 55(8–9):1164–86. PMID: 10442095
 32. Chan S, Yan C. PDE1 isozymes, key regulators of pathological vascular remodeling. *Curr Opin Pharmacol*. 2011; 11(6):720–4. <https://doi.org/10.1016/j.coph.2011.09.002> PMID: 21962439
 33. Kusano E, Yoshida I, Takeda S, Homma S, Yusufi AN, Dousa TP, et al. Nephron distribution of total low Km cyclic AMP phosphodiesterase in mouse, rat and rabbit kidney. *Tohoku J Exp Med*. 2001; 193(3):207–20. PMID: 11315768
 34. Kurihara I, Saito T, Obara K, Shoji Y, Hirai M, Soma J, et al. Effect of a nonpeptide vasopressin V1 antagonist (OPC-21268) on experimental accelerated focal glomerulosclerosis. *Nephron*. 1996; 73(4):629–36. PMID: 8856262
 35. Whitfield JF, MacManus JP, Gillan DJ. The ability of calcium to change cyclic AMP from a stimulator to an inhibitor to thymic lymphoblast proliferation. *J Cell Physiol*. 1973; 81(2):241–50. <https://doi.org/10.1002/jcp.1040810212> PMID: 4348556
 36. Dumaz N, Marais R. Integrating signals between cAMP and the RAS/RAF/MEK/ERK signalling pathways—Based on the Anniversary Prize of the Gesellschaft für Biochemie und Molekularbiologie Lecture delivered on 5 July 2003 at the special FEBS meeting in Brussels. *FEBS J*. 2005; 272(14):3491–504. <https://doi.org/10.1111/j.1742-4658.2005.04763.x> PMID: 16008550
 37. Stork PJ, Schmitt JM. Crosstalk between cAMP and MAP kinase signaling in the regulation of cell proliferation. *Trends Cell Biol*. 2002; 12(6):258–66. PMID: 12074885
 38. Yamaguchi T, Pelling J, Ramaswamy N, Eppler J, Wallace D, Nagao S, et al. cAMP stimulates the *in vitro* proliferation of renal cyst epithelial cells by activating the extracellular signal-regulated kinase pathway. *Kidney Int*. 2000; 57(4):1460–71. <https://doi.org/10.1046/j.1523-1755.2000.00991.x> PMID: 10760082
 39. Hanaoka K, Guggino W. cAMP regulates cell proliferation and cyst formation in autosomal polycystic kidney disease cells. *J Am Soc Nephrol*. 2000; 11:1179–87. PMID: 10864573
 40. Yamaguchi T, Nagao S, Wallace DP, Belibi FA, Cowley BD, Pelling JC, et al. Cyclic AMP activates B-Raf and ERK in cyst epithelial cells from autosomal-dominant polycystic kidneys. *Kidney Int*. 2003; 63(6):1983–94. <https://doi.org/10.1046/j.1523-1755.2003.00023.x> PMID: 12753285

41. Chini CC, Grande JP, Chini EN, Dousa TP. Compartmentalization of cAMP signaling in mesangial cells by phosphodiesterase isozymes PDE3 and PDE4. Regulation of superoxidation and mitogenesis. *J Biol Chem*. 1997; 272(15):9854–9. PMID: [9092521](#)
42. Cheng J, Thompson MA, Walker HJ, Gray CE, Diaz Encarnacion MM, Warner GM, et al. Differential regulation of mesangial cell mitogenesis by cAMP phosphodiesterase isozymes 3 and 4. *Am J Physiol Renal Physiol*. 2004; 287(5):F940–53. <https://doi.org/10.1152/ajprenal.00079.2004> PMID: [15280158](#)
43. Osinski MT, Schror K. Inhibition of platelet-derived growth factor-induced mitogenesis by phosphodiesterase 3 inhibitors: role of protein kinase A in vascular smooth muscle cell mitogenesis. *Biochem Pharmacol*. 2000; 60(3):381–7. PMID: [10856433](#)
44. Matousovic K, Tsuboi Y, Walker H, Grande JP, Dousa TP. Inhibitors of cyclic nucleotide phosphodiesterase isozymes block renal tubular cell proliferation induced by folic acid. *J Lab Clin Med*. 1997; 130(5):487–95. PMID: [9390636](#)
45. Cheng J, Thompson MA, Walker HJ, Gray CE, Warner GM, Zhou W, et al. Lixazinone stimulates mitogenesis of Madin-Darby canine kidney cells. *Exp Biol Med (Maywood)*. 2006; 231(3):288–95.
46. Rybalkin SD, Rybalkina I, Beavo JA, Bornfeldt KE. Cyclic nucleotide phosphodiesterase 1C promotes human arterial smooth muscle cell proliferation. *Circ Res*. 2002; 90(2):151–7. PMID: [11834707](#)
47. Nagel DJ, Aizawa T, Jeon KI, Liu W, Mohan A, Wei H, et al. Role of nuclear Ca²⁺/calmodulin-stimulated phosphodiesterase 1A in vascular smooth muscle cell growth and survival. *Circ Res*. 2006; 98(6):777–84. <https://doi.org/10.1161/01.RES.0000215576.27615.f0> PMID: [16514069](#)
48. Cai Y, Nagel DJ, Zhou Q, Cygnar KD, Zhao H, Li F, et al. Role of cAMP-phosphodiesterase 1C signaling in regulating growth factor receptor stability, vascular smooth muscle cell growth, migration, and neointimal hyperplasia. *Circ Res*. 2015; 116(7):1120–32. <https://doi.org/10.1161/CIRCRESAHA.116.304408> PMID: [25608528](#)
49. Sussman CR, Chowdhury RB, Duran MT, Harris PC, Torres VE, editors. Morpholino and mutant studies of Pde3A and Pde1a in renal cystogenesis using zebrafish. *American Society of Nephrology Kidney Week*; 2015; San Diego, CA.
50. Pinto CS, Raman A, Reif GA, Magenheimer BS, White C, Calvet JP, et al. Phosphodiesterase Isoform Regulation of Cell Proliferation and Fluid Secretion in Autosomal Dominant Polycystic Kidney Disease. *J Am Soc Nephrol*. 2016; 27(4):1124–34. <https://doi.org/10.1681/ASN.2015010047> PMID: [26289612](#)
51. Mutig K, Paliege A, Kahl T, Jons T, Muller-Esterl WP, Bachmann S. Vasopressin V2 receptor expression along rat, mouse, and human renal epithelia with focus on TAL. *Am J Physiol Renal Physiol*. 2007; 293:F1166–F77. <https://doi.org/10.1152/ajprenal.00196.2007> PMID: [17626156](#)
52. Sarmiento JM, Ehrenfeld P, Anazco CC, Reyes CE, Troncoso S, Figueroa CD, et al. Differential distribution of the vasopressin V receptor along the rat nephron during renal ontogeny and maturation. *Kidney Int*. 2005; 68(2):487–96. <https://doi.org/10.1111/j.1523-1755.2005.00426.x> PMID: [16014025](#)
53. O'Sullivan DA, Torres VE, Edwards WD, Edwards BS, Griffin MD, Cai Y, et al. Cardiac expression of polycystin 1 and polycystin 2 and idiopathic dilated cardiomyopathy in autosomal dominant polycystic kidney disease (ADPKD). *J Am Soc Nephrol*. 1997; 8:376A.
54. Volk T, Schwoerer AP, Thiessen S, Schultz JH, Ehmke H. A polycystin-2-like large conductance cation channel in rat left ventricular myocytes. *Cardiovasc Res*. 2003; 58(1):76–88. PMID: [12667948](#)
55. Griffin MD, Torres VE, Grande JP, Kumar R. Vascular expression of polycystin. *J Am Soc Nephrol*. 1997; 8:616–26. PMID: [10495791](#)
56. Torres VE, Cai Y, Chen X, Wu GQ, Geng L, Cleghorn KA, et al. Vascular expression of polycystin 2. *J Am Soc Nephrol*. 2001; 12:1–9. PMID: [11134244](#)
57. Paavola J, Schliffke S, Rossetti S, Kuo IY, Yuan S, Sun Z, et al. Polycystin-2 mutations lead to impaired calcium cycling in the heart and predispose to dilated cardiomyopathy. *J Mol Cell Cardiol*. 2013; 58:199–208. <https://doi.org/10.1016/j.yjmcc.2013.01.015> PMID: [23376035](#)
58. Kuo IY, Kwaczala AT, Nguyen L, Russell KS, Campbell SG, Ehrlich BE. Decreased polycystin 2 expression alters calcium-contraction coupling and changes beta-adrenergic signaling pathways. *Proc Natl Acad Sci U S A*. 2014; 111(46):16604–9. <https://doi.org/10.1073/pnas.1415933111> PMID: [25368166](#)
59. Balbo BE, Amaral AG, Fonseca JM, de Castro I, Salemi VM, Souza LE, et al. Cardiac dysfunction in Pkd1-deficient mice with phenotype rescue by galectin-3 knockout. *Kidney Int*. 2016; 90(3):580–97. <https://doi.org/10.1016/j.kint.2016.04.028> PMID: [27475230](#)
60. Pedrozo Z, Criollo A, Battiprolu PK, Morales CR, Contreras-Ferrat A, Fernandez C, et al. Polycystin-1 Is a Cardiomyocyte Mechanosensor That Governs L-Type Ca²⁺ Channel Protein Stability. *Circulation*. 2015; 131(24):2131–42. <https://doi.org/10.1161/CIRCULATIONAHA.114.013537> PMID: [25888683](#)
61. Kokkonen K, Kass DA. Nanodomain Regulation of Cardiac Cyclic Nucleotide Signaling by Phosphodiesterases. *Annu Rev Pharmacol Toxicol*. 2016.

62. Bode DC, Kanter JR, Brunton LL. Cellular distribution of phosphodiesterase isoforms in rat cardiac tissue. *Circ Res*. 1991; 68(4):1070–9. PMID: [1849058](#)
63. Kostic MM, Erdogan S, Rena G, Borchert G, Hoch B, Bartel S, et al. Altered expression of PDE1 and PDE4 cyclic nucleotide phosphodiesterase isoforms in 7-oxo-prostacyclin-preconditioned rat heart. *J Mol Cell Cardiol*. 1997; 29(11):3135–46. <https://doi.org/10.1006/jmcc.1997.0544> PMID: [9405187](#)
64. Sonnenburg WK, Rybalkin SD, Bornfeldt KE, Kwak KS, Rybalkina IG, Beavo JA. Identification, quantitation, and cellular localization of PDE1 calmodulin-stimulated cyclic nucleotide phosphodiesterases. *Methods*. 1998; 14(1):3–19. <https://doi.org/10.1006/meth.1997.0561> PMID: [9500854](#)
65. Wallis RM, Corbin JD, Francis SH, Ellis P. Tissue distribution of phosphodiesterase families and the effects of sildenafil on tissue cyclic nucleotides, platelet function, and the contractile responses of trabeculae carneae and aortic rings in vitro. *Am J Cardiol*. 1999; 83(5A):3C–12C. PMID: [10078537](#)
66. Hambleton R, Krall J, Tikishvili E, Honegger M, Ahmad F, Manganiello VC, et al. Isoforms of cyclic nucleotide phosphodiesterase PDE3 and their contribution to cAMP hydrolytic activity in subcellular fractions of human myocardium. *J Biol Chem*. 2005; 280(47):39168–74. <https://doi.org/10.1074/jbc.M506760200> PMID: [16172121](#)
67. Vandeput F, Wolda SL, Krall J, Hambleton R, Uher L, McCaw KN, et al. Cyclic nucleotide phosphodiesterase PDE1C1 in human cardiac myocytes. *J Biol Chem*. 2007; 282(45):32749–57. <https://doi.org/10.1074/jbc.M703173200> PMID: [17726023](#)
68. Miller CL, Oikawa M, Cai Y, Wojtovich AP, Nagel DJ, Xu X, et al. Role of Ca²⁺/calmodulin-stimulated cyclic nucleotide phosphodiesterase 1 in mediating cardiomyocyte hypertrophy. *Circ Res*. 2009; 105(10):956–64. <https://doi.org/10.1161/CIRCRESAHA.109.198515> PMID: [19797176](#)
69. Mokni W, Keravis T, Etienne-Selloum N, Walter A, Kane MO, Schini-Kerth VB, et al. Concerted regulation of cGMP and cAMP phosphodiesterases in early cardiac hypertrophy induced by angiotensin II. *PLoS One*. 2010; 5(12):e14227. <https://doi.org/10.1371/journal.pone.0014227> PMID: [21151982](#)
70. Lakics V, Karran EH, Boess FG. Quantitative comparison of phosphodiesterase mRNA distribution in human brain and peripheral tissues. *Neuropharmacology*. 2010; 59(6):367–74. <https://doi.org/10.1016/j.neuropharm.2010.05.004> PMID: [20493887](#)
71. Miller CL, Cai Y, Oikawa M, Thomas T, Dostmann WR, Zaccolo M, et al. Cyclic nucleotide phosphodiesterase 1A: a key regulator of cardiac fibroblast activation and extracellular matrix remodeling in the heart. *Basic Res Cardiol*. 2011; 106(6):1023–39. <https://doi.org/10.1007/s00395-011-0228-2> PMID: [22012077](#)
72. Johnson WB, Katugampola S, Able S, Napier C, Harding SE. Profiling of cAMP and cGMP phosphodiesterases in isolated ventricular cardiomyocytes from human hearts: comparison with rat and guinea pig. *Life Sci*. 2012; 90(9–10):328–36. <https://doi.org/10.1016/j.lfs.2011.11.016> PMID: [22261303](#)
73. Knight WE, Chen S, Zhang Y, Oikawa M, Wu M, Zhou Q, et al. PDE1C deficiency antagonizes pathological cardiac remodeling and dysfunction. *Proc Natl Acad Sci U S A*. 2016.
74. Lukyanenko YO, Younes A, Lyashkov AE, Tarasov KV, Riordon DR, Lee J, et al. Ca²⁺/calmodulin-activated phosphodiesterase 1A is highly expressed in rabbit cardiac sinoatrial nodal cells and regulates pacemaker function. *J Mol Cell Cardiol*. 2016; 98:73–82. <https://doi.org/10.1016/j.yjmcc.2016.06.064> PMID: [27363295](#)
75. Jeon KI, Jono H, Miller CL, Cai Y, Lim S, Liu X, et al. Ca²⁺/calmodulin-stimulated PDE1 regulates the beta-catenin/TCF signaling through PP2A B56 gamma subunit in proliferating vascular smooth muscle cells. *Febs J*. 2010; 277(24):5026–39. <https://doi.org/10.1111/j.1742-4658.2010.07908.x> PMID: [21078118](#)
76. Tragante V, Barnes MR, Ganesh SK, Lanktree MB, Guo W, Franceschini N, et al. Gene-centric meta-analysis in 87,736 individuals of European ancestry identifies multiple blood-pressure-related loci. *Am J Hum Genet*. 2014; 94(3):349–60. <https://doi.org/10.1016/j.ajhg.2013.12.016> PMID: [24560520](#)
77. Boda H, Uchida H, Takaiso N, Ouchi Y, Fujita N, Kuno A, et al. A PDE3A mutation in familial hypertension and brachydactyly syndrome. *J Hum Genet*. 2016; 61(8):701–3. <https://doi.org/10.1038/jhg.2016.32> PMID: [27053290](#)
78. Ortiz-Capisano MC, Liao TD, Ortiz PA, Beierwaltes WH. Calcium-dependent phosphodiesterase 1C inhibits renin release from isolated juxtaglomerular cells. *Am J Physiol Regul Integr Comp Physiol*. 2009; 297(5):R1469–76. <https://doi.org/10.1152/ajpregu.00121.2009> PMID: [19741056](#)
79. Friis UG, Madsen K, Stubbe J, Hansen PB, Svenningsen P, Bie P, et al. Regulation of renin secretion by renal juxtaglomerular cells. *Pflugers Arch*. 2013; 465(1):25–37. <https://doi.org/10.1007/s00424-012-1126-7> PMID: [22733355](#)
80. Yu TM, Chuang YW, Yu MC, Huang ST, Chou CY, Lin CL, et al. New-onset Atrial Fibrillation is Associated With Polycystic Kidney Disease: A Nationwide Population-based Cohort Study. *Medicine (Baltimore)*. 2016; 95(4):e2623.

81. Bobin P, Belacel-Ouari M, Bedioune I, Zhang L, Leroy J, Leblais V, et al. Cyclic nucleotide phosphodiesterases in heart and vessels: A therapeutic perspective. *Arch Cardiovasc Dis.* 2016; 109(6–7):431–43. <https://doi.org/10.1016/j.acvd.2016.02.004> PMID: 27184830